

Received December 5, 2018, accepted January 6, 2019, date of publication January 24, 2019, date of current version February 27, 2019.

Digital Object Identifier 10.1109/ACCESS.2019.2894774

Heterogeneous-Objective Robust Optimization of Complex Mechatronic Components Considering Interval Uncertainties

JIN CHENG^{1,2}, YANGMING QIAN^{1,2}, ZHENYU LIU¹, YIXIONG FENG¹, (Member, IEEE), ZHENDONG ZHOU^{1,2}, AND JIANRONG TAN¹

¹State Key Laboratory of Fluid Power and Mechatronic Systems, Zhejiang University, Hangzhou 310027, China

²Key Laboratory of Micro-Systems and Micro-Structures Manufacturing, Ministry of Education, Harbin Institute of Technology, Harbin 150080, China

Corresponding authors: Zhenyu Liu (liuzy@zju.edu.cn) and Yixiong Feng (fyxtv@zju.edu.cn)

This work was supported in part by the National Natural Science Foundation of China under Grant 51775491 and Grant 51821093, in part by the National Key Research and Development Project of China under Grant 2017YFB0603704, in part by the Key Laboratory of Micro-Systems and Micro-Structures Manufacturing, Ministry of Education, Harbin Institute of Technology, under Grant 2015KM001, and in part by the Fundamental Research Funds for the Central Universities.

ABSTRACT Structural optimization of complex mechatronic components may involve heterogeneous competing performance indices, including the cost, fixation, benefit, and deviation ones. However, such optimization problems with heterogeneous objectives have not been investigated so far. In this paper, a novel interval heterogeneous-objective robust optimization approach is proposed for complex mechatronic components. First, a unified interval heterogeneous-objective robust optimization model is constructed for mechatronic components with the uncertainties described as interval variables. Subsequently, a new interval robust equilibrium optimization algorithm is proposed to solve the interval heterogeneous-objective robust optimization model. Specifically, the unified formulas for assessing the robustness of interval heterogeneous-objective performance indices and the robust equilibrium among them are derived at first. Then, the preferential guidelines considering the robust equilibrium among all the objective and constraint performance indices are proposed for the direct ranking of various design vectors, and finally, the heterogeneous-objective robust equilibrium optimization of complex mechatronic components is realized by integrating the Kriging technique and the nested genetic algorithm. The feasibility and effectiveness of the proposed heterogeneous-objective robust optimization approach are verified by a numerical example and a case study.

INDEX TERMS Heterogeneous-objective robust optimization, complex mechatronic component, interval, robust equilibrium, closeness coefficient, group ranking.

I. INTRODUCTION

Uncertainties such as machining and assembly errors, material variations of key components, voltage fluctuations, and so on are inevitable for complex mechatronic equipment. The optimal designs for the key components of complex mechatronic equipment obtained by traditional deterministic optimization approaches neglecting these uncertainties can hardly achieve the desired structural performance and may be sensitive to uncertainties. Therefore, it is necessary for us to take these uncertainties into consideration in the design process of complex mechatronic components [1]–[4].

Robust design optimization capable of achieving the design of optimal structural performance insensitive to uncertainties by combining the optimization theory with robustness

assessment has been widely applied in engineering [5]–[10]. Traditional robust design of uncertain structures is usually conducted on the premise that the probabilistic distributions of uncertainties are known [11]. For example, Medina and Taflanidis [12] proposed a probabilistic robustness measure defined as the likelihood that a particular design outperformed the rival ones in an alternative set. Richardson *et al.* [13] investigated the robust topology optimization of truss structures with random loads and material properties. Cheng *et al.* [14] investigated the robust optimization of dynamical characteristics for complex structures with random parameters by integrating Kriging technique and the constrained non-dominated sorting genetic algorithm. Martínez-Frutos *et al.* [15] proposed a stochastic robust shape

optimization framework for continuous structures based on the level set method. Zhang and Kang [16] investigated the robust shape and topology optimization method considering geometrical uncertainties with stochastic level set perturbation. However, the precise probabilistic distributions of uncertainties can hardly be determined in the design phase of complex mechatronic components due to the lack of uncertain information [17]–[25].

In recent years, a series of non-probabilistic robust optimization approaches have been proposed [26], [27]. For instance, Gong *et al.* [28] proposed a set-based genetic algorithm for interval many-objective optimization problems. Sun *et al.* [29] put forward an ensemble framework for assessing solutions of interval programming problems. Zhou *et al.* [30] proposed a sequential quadratic programming approach for robust optimization with interval uncertainties. Mortazavi *et al.* [31] investigated the adaptive gradient-assisted robust design optimization under interval uncertainty. Cheng *et al.* [32] proposed a hybrid algorithm for multi-objective robust optimization with interval uncertainty by integrating multi-objective differential evolution, sequential quadratic programming with robust optimization. Wu *et al.* [33] investigated the robust topology optimization of structures under interval uncertainty and developed a new sensitivity analysis method. Chen *et al.* [34] proposed the target-performance-based analytical scheme for the robust optimization of uncertain structures based on hyper-ellipsoidal and interval models. Hot *et al.* [35] investigated the robust design of a pre-stressed space structure under epistemic uncertainties based on info-gap model. Hanks *et al.* [36] proposed a robust goal programming approach utilizing different robustness echelons via the norm-based and ellipsoidal uncertainty sets. Cheng *et al.* [37] proposed an efficient robust optimization approach for complex uncertain structures based on normalized violation degrees of interval constraints. Hu *et al.* [38] investigated the robust optimization with convex model considering bounded constraints and proposed a new robustness index based on the sensitivity Jacobian matrix of system performances. Liu and Gea [39] put forward a new robust topology optimization approach for structures under multiple independent unknown-but-bounded loads based on the Wolfe duality. Zhou *et al.* [40]–[42] proposed an on-line Kriging model-assisted variable adjustment robust optimization approach and the multi-objective robust optimization approach for engineering design under interval uncertainty.

As can be seen from the above literature review, the present researches on non-probabilistic robust optimization have the following limitations. Firstly, most of them are focused on the problem of single objective optimization and cannot handle the robust optimization problems with multiple objective performance indices. Secondly, present multi-objective non-probabilistic robust optimization approaches usually produce a set of Pareto-optimal solutions. The determination of a final design from Pareto optimal solutions is a challenging task dependent on the rich experience and expert skills of decision

makers, which greatly limits the application of present multi-objective robust optimization approaches in engineering. Gong and Yuan [43] and Gong *et al.* [44] proposed evolutionary algorithms with preference polyhedron and interactive evolutionary algorithms with decision-maker's preferences for solving interval multi-objective optimization problems, which generated one or more preferred Pareto-optimal solutions and thus reduced the difficulty of decision making after optimization. They provided the valuable idea of introducing decision making into the optimization process, which also applies to interval multi-objective robust optimization. Finally, all of the present researches on robust optimization are focused on the problems with only cost or benefit objective functions, the goal of which is to minimize or maximize the objective values and reduce their sensitivity to uncertainties. However, the optimization of complex mechatronic components may simultaneously involve the cost, fixation, benefit and deviation objective performance indices [45]. Namely, there may be the cost objective that is the smaller the better, the fixation objective that is the closer to a given constant the better, the benefit objective that is the larger the better, and the deviation objective that is the farther away from a given constant the better. Take the high-speed actuating mechanism as an example, the maximum deformation is a cost performance index since the smaller deformation indicates the higher stiffness; the maximum equivalent stress can be regarded as a fixation performance index considering its given upper limit and the purpose of avoiding over-conservative design [46]; the stamping frequency is a benefit performance index since it is the larger the better; the natural frequency can be regarded as a deviation performance index since its farther distance from the stamping frequency indicates the better anti-vibration performance of the mechanism. Whereas the robust optimization problem with heterogeneous objectives has not been investigated so far, which is much more difficult to solve compared with the conventional multi-objective robust optimization problems due to the competition among heterogeneous objectives.

In this paper, the new research topic of interval heterogeneous-objective robust optimization is investigated for the first time. A novel heterogeneous-objective robust optimization approach is proposed for complex uncertain mechatronic components. A unified interval heterogeneous-objective robust optimization model is constructed for complex mechatronic components with the uncertainties influencing structural performance indices described as interval variables. To avoid the challenging decision-making process of choosing the final design from Pareto optimal solutions, the interval heterogeneous-objective robust optimization model is solved by a novel interval robust equilibrium optimization algorithm considering the conflict and competition among all the objective and constraint performance indices. Firstly, the unified formulae for assessing the robustness of heterogeneous objective performance indices as well as the robust equilibrium among them are derived. Secondly, the preferential guidelines considering

the robust equilibrium among all the objective and constraint performance indices are put forward for directly ranking various design vectors based on grouping and group ranking. Finally, the interval heterogeneous-objective robust equilibrium optimization algorithm is realized by integrating Kriging technique and nested genetic algorithm (GA). As a result, the optimal solution to the interval heterogeneous-objective robust optimization model can be located with no challenging decision-making process involved. The feasibility and validity of the proposed heterogeneous-objective robust optimization approach are verified by both numerical example and case study.

II. UNIFIED INTERVAL HETEROGENEOUS-OBJECTIVE ROBUST OPTIMIZATION MODEL FOR COMPLEX UNCERTAIN MECHATRONIC COMPONENTS

An interval number U can be denoted as

$$U = [u^L, u^R] = \langle u^C, u^W \rangle, \quad (1)$$

where u^L, u^R, u^C, u^W are its left bound, right bound, center and width. And there are

$$u^C = (u^L + u^R)/2, \quad (2)$$

$$u^W = u^R - u^L. \quad (3)$$

Robust optimization of complex uncertain mechatronic components may involve heterogeneous objectives including the cost, fixation, benefit and deviation structural performance indices, which are the functions of design variables and interval parameters when the uncertainties are described as interval numbers. Supposing that the cost, fixation and deviation structural performance indices are indicated by subscripts 1, 2, 3, 4 respectively, the heterogeneous objectives involved in the robust optimization of an uncertain mechatronic component can be described as

$$\min_x \left\{ f_{1i}^C(\mathbf{x}), f_{1i}^W(\mathbf{x}) \right\} \quad (i = 1, 2, \dots, n1); \quad (4)$$

$$\min_x \left\{ \left| f_{2i}^C(\mathbf{x}) - b_{2i}^C \right|, f_{2i}^W(\mathbf{x}) \right\} \quad (i = 1, 2, \dots, n2); \quad (5)$$

$$\min_x \left\{ -f_{3i}^C(\mathbf{x}), f_{3i}^W(\mathbf{x}) \right\} \quad (i = 1, 2, \dots, n3); \quad (6)$$

$$\min_x \left\{ -\left| f_{4i}^C(\mathbf{x}) - b_{4i}^C \right|, f_{4i}^W(\mathbf{x}) \right\} \quad (i = 1, 2, \dots, n4). \quad (7)$$

where \mathbf{x} is the design vector of a mechatronic component; $f_{1i}^C(\mathbf{x}), f_{1i}^W(\mathbf{x}), f_{2i}^C(\mathbf{x}), f_{2i}^W(\mathbf{x}), f_{3i}^C(\mathbf{x}), f_{3i}^W(\mathbf{x}), f_{4i}^C(\mathbf{x}), f_{4i}^W(\mathbf{x})$ are the center and width of the cost, fixation, benefit and deviation structural performance indices respectively; $n1, n2, n3, n4$ are the numbers of the cost, fixation, benefit and deviation performance indices; subscript i indicates the i th objective performance index in the same category; b_{2i}^C is the center of the i th interval constant B_{2i} that the i th fixation performance index is expected to approach; b_{4i}^C is the center of the i th interval constant B_{4i} that the i th deviation performance index is expected to deviate from.

Supposing that all the structural performance indices of an uncertain mechatronic component are influenced by both

design variables and interval uncertain parameters and that there are some performance indices with upper limits besides the heterogeneous ones, the interval robust optimization model of an uncertain mechatronic component with heterogeneous objective performance indices can be unified as

$$\min_x \left\{ \left(\text{sign}(2.5 - j) \times \left(f_{ji}^C(\mathbf{x}) / \left| f_{ji}^C(\mathbf{x}) \right| \right)^j \times \left| f_{ji}^C(\mathbf{x}) - b_{ji}^C \right|, f_{ji}^W(\mathbf{x}) \right) \right\},$$

where

$$f_{ji}^C(\mathbf{x}) = (f_{ji}^L(\mathbf{x}) + f_{ji}^R(\mathbf{x})) / 2, \quad f_{ji}^W(\mathbf{x}) = f_{ji}^R(\mathbf{x}) - f_{ji}^L(\mathbf{x});$$

$$f_{ji}^L(\mathbf{x}) = \min_U f_{ji}(\mathbf{x}, U), \quad f_{ji}^R(\mathbf{x}) = \max_U f_{ji}(\mathbf{x}, U);$$

$$B_{ji} = [b_{ji}^L, b_{ji}^R] = \langle b_{ji}^C, b_{ji}^W \rangle;$$

$$B_{1i} = B_{3i} = [0, 0] = \langle 0, 0 \rangle;$$

$$i = \begin{cases} 1, 2, \dots, n1. & j = 1; \\ 1, 2, \dots, n2. & j = 2; \\ 1, 2, \dots, n3. & j = 3; \\ 1, 2, \dots, n4. & j = 4. \end{cases}$$

$$\text{s.t. } G_k(\mathbf{x}) \leq B_k \quad (k = 1, 2, \dots, ng). \quad (8)$$

where

$$G_k(\mathbf{x}) = g_k(\mathbf{x}, U) = [g_k^L(\mathbf{x}), g_k^R(\mathbf{x})] = \langle g_k^C(\mathbf{x}), g_k^W(\mathbf{x}) \rangle;$$

$$g_k^L(\mathbf{x}) = \min_U g_k(\mathbf{x}, U), \quad g_k^R(\mathbf{x}) = \max_U g_k(\mathbf{x}, U);$$

$$g_k^C(\mathbf{x}) = (g_k^L(\mathbf{x}) + g_k^R(\mathbf{x})) / 2, \quad g_k^W(\mathbf{x}) = g_k^R(\mathbf{x}) - g_k^L(\mathbf{x});$$

$$B_k = [b_k^L, b_k^R] = \langle b_k^C, b_k^W \rangle;$$

$$\mathbf{x} = (x_1, x_2, \dots, x_{nx}), \quad x_l \in [x_l^L, x_l^R] \quad (l = 1, 2, \dots, nx);$$

$$U = (U_1, U_2, \dots, U_{nu}),$$

$$U_m = [u_m^L, u_m^R] \quad (m = 1, 2, \dots, nu).$$

where \mathbf{x} is an nx -dimensional design vector, U is an nu -dimensional interval parameter vector. $f_{ji}(\mathbf{x}, U)$ and $G_k(\mathbf{x})$ are the objective and constraint performance indices of the uncertain mechatronic component, which are the functions of design vector \mathbf{x} and interval parameter vector U . $f_{ji}^C(\mathbf{x}), f_{ji}^W(\mathbf{x}), f_{ji}^L(\mathbf{x})$ and $f_{ji}^R(\mathbf{x})$ are the center, width, left and right bounds of the i th objective performance index in the j th category of heterogeneous objectives. $g_k^L(\mathbf{x}), g_k^R(\mathbf{x}), g_k^C(\mathbf{x})$ and $g_k^W(\mathbf{x})$ are the left bound, right bound, center and width of the k th constraint performance index. B_k is the given interval constant corresponding to the k th constraint performance index while $b_k^L, b_k^R, b_k^C, b_k^W$ are its left bound, right bound, center and width. It is worth noting that the objective functions in (8) are the same as (4), (5), (6), (7) respectively when j equals 1, 2, 3, 4.

III. UNIFIED ASSESSMENT OF ROBUST EQUILIBRIUM AMONG HETEROGENEOUS OBJECTIVES

The optimal solution to the interval heterogeneous objective robust optimization problem in (8) should have robust

$$Rf_{ji}(\mathbf{x}) = \frac{|\text{sign}(j-2)| \times |f_{ji}^C(\mathbf{x}) - b_{ji}^C| + |\text{sign}[(j-1) \times (j-3) \times (j-4)]| \times |f_{ji}^W(\mathbf{x}) - b_{ji}^W|}{|f_{ji}^C(\mathbf{x}) - b_{ji}^C| + |f_{ji}^W(\mathbf{x}) - b_{ji}^W|} \quad (12)$$

equilibrium structural performance indices considering the conflict and competition among them. That is, all the structural performance indices of the optimal solution should have approximate values of robustness indices.

To assess the robust equilibrium among heterogeneous objectives, the robustness of heterogeneous objective performance indices $f_{ji}(\mathbf{x}, \mathbf{U}) = F_{ji}(\mathbf{x})$ ($j = 1, 2, 3, 4$) should be assessed at first. This section firstly proposes the formulae for assessing the robustness of the cost, benefit, fixation and deviation performance indices, then derives the unified formula for assessing the robustness of all heterogeneous objective performance indices, and finally proposes the approach for assessing the robust equilibrium among heterogeneous objective performance indices.

A. UNIFIED ROBUST ASSESSMENT OF HETEROGENEOUS OBJECTIVE PERFORMANCE INDICE

For a cost or benefit performance index $F_{ji}(\mathbf{x})$ ($j = 1, 3$), the larger fluctuation under uncertainties indicates the worse robustness. Thus the robustness of a cost or benefit performance index can be assessed by

$$Rf_{ji}(\mathbf{x}) = \frac{|f_{ji}^C(\mathbf{x})|}{|f_{ji}^C(\mathbf{x})| + |f_{ji}^W(\mathbf{x})|} \quad (j = 1, 3). \quad (9)$$

For a fixation performance index $F_{2i}(\mathbf{x})$, the larger deviation from given interval constant B_{2i} indicates the worse robustness. Considering that two fixation performance indices symmetrical about B_{2i} have the same robust level, the robustness of a fixation performance index can be assessed by

$$Rf_{2i}(\mathbf{x}) = \frac{|f_{2i}^W(\mathbf{x}) - b_{2i}^W|}{|f_{2i}^W(\mathbf{x}) - b_{2i}^W| + |f_{2i}^C(\mathbf{x}) - b_{2i}^C|}. \quad (10)$$

For a deviation performance index $F_{4i}(\mathbf{x})$, the larger deviation from given interval constant B_{4i} indicates the better robustness, which is just opposite to a fixation one. Thus the robustness of a deviation performance index can be evaluated by

$$Rf_{4i}(\mathbf{x}) = \frac{|f_{4i}^C(\mathbf{x}) - b_{4i}^C|}{|f_{4i}^W(\mathbf{x}) - b_{4i}^W| + |f_{4i}^C(\mathbf{x}) - b_{4i}^C|}. \quad (11)$$

Considering that there are $B_{1i} = B_{3i} = \langle 0, 0 \rangle$ for the cost and benefit performance indices, the formula for assessing the robustness of heterogeneous objective performance indices including the cost, fixation, benefit and deviation ones can be unified as (12) shown at the top of this page. Obviously, there is $0 \leq Rf_{ji}(\mathbf{x}) \leq 1$ for any objective performance index. The larger objective robustness index $Rf_{ji}(\mathbf{x})$ indicates the better robustness of objective performance index $F_{ji}(\mathbf{x})$.

B. UNIFIED ASSESSMENT OF ROBUST EQUILIBRIUM AMONG HETEROGENEOUS OBJECTIVES

To assess the robust equilibrium among heterogeneous objective performance indices, the robust equilibrium coefficient for design vector \mathbf{x} as far as the i th objective performance index in category j can be calculated by

$$Bf_{ji}(\mathbf{x}) = Rf_{ji}(\mathbf{x}) - \overline{Rf_{ji}(\mathbf{x})} \quad (13)$$

where $\overline{Rf_{ji}(\mathbf{x})}$ is the average of the i th objective performance index in category j for a group of alternative design vectors.

Then the heterogeneous objective performance indices are robust equilibrium for design vector \mathbf{x} if there is $\forall Bf_{ji}(\mathbf{x}) \geq 0$; otherwise, they are not. Design vector \mathbf{x}_1 has the more robust equilibrium objective performance indices than design vector \mathbf{x}_2 if there is $\forall Bf_{ji}(\mathbf{x}_1) \geq 0$ but $\exists Bf_{ji}(\mathbf{x}_2) < 0$.

IV. PREFERENTIAL GUIDELINES FOR DESIGN VECTORS OF UNCERTAIN MECHATRONIC COMPONENTS

In order to realize the direct ranking of design vectors and locate the robust optimal solution to the heterogeneous-objective robust optimization problem in (8), the preferential guidelines for design vectors of uncertain mechatronic components are put forward based on grouping and group ranking. Firstly, all the alternative design vectors are classified into two groups (namely, the feasible and infeasible ones) according to the results of feasibility assessment. Secondly, the feasible design vectors are further classified into four groups according to the robust equilibrium among all of their structural performance indices. Finally, the rank orders of all the alternative design vectors are determined by group ranking after ranking in each group.

A. FEASIBILITY ASSESSMENT OF DESIGN VECTORS AND RANKING OF INFEASIBLE ONES

According to the frequency that the boundaries of constraint performance index $G_k(\mathbf{x})$ in (8) cross over those of its corresponding interval constant B_k , there are five positional relationships between $G_k(\mathbf{x})$ and B_k : (a) no boundary crossing as shown in Fig. 1(a); (b) one boundary crossing, namely, $g_k^R(\mathbf{x})$ crosses over b_k^L as shown in Fig. 1(b); (c) two boundary crossings, namely, $g_k^R(\mathbf{x})$ crosses over both b_k^L and b_k^R when $g_k^W(\mathbf{x}) > b_k^W$ as shown in Fig. 1(c₁) or both $g_k^R(\mathbf{x})$ and $g_k^L(\mathbf{x})$ cross over b_k^L when $g_k^W(\mathbf{x}) < b_k^W$ as shown in Fig. 1(c₂); (d) three boundary crossings, namely, $g_k^R(\mathbf{x})$ crosses over both b_k^L and b_k^R while $g_k^L(\mathbf{x})$ crosses over b_k^L , see Fig. 1(d); (e) four boundary crossings, namely, both $g_k^R(\mathbf{x})$ and $g_k^L(\mathbf{x})$ cross over b_k^L and b_k^R , see Fig. 1(e).

To describe the relative position between interval constraint performance index $G_k(\mathbf{x})$ and interval constant B_k ,

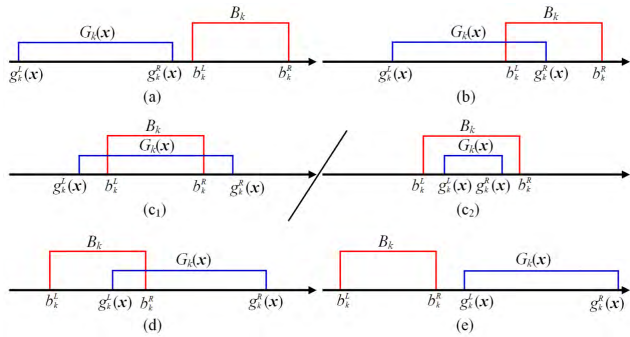


FIGURE 1. Relative positional relationships between interval performance index $G_k(x)$ and interval constant B_k .

a new concept of closeness coefficient is proposed. Specifically, a closeness coefficient describes the degree that the boundary of interval constraint performance index $G_k(x)$ approaches that of interval constant B_k , which monotonously increases from 0 to 1 when the former gradually approaches the latter and keeps the value of 1 after the former crosses the latter.

There are four closeness coefficients for describing the relative position between interval performance index $G_k(x)$ and constant B_k , namely, $cc_k^{RL}(x)$ describing the degree of $g_k^R(x)$ approaching b_k^L , $cc_k^{LL}(x)$ describing the degree of $g_k^L(x)$ approaching b_k^L , $cc_k^{RR}(x)$ describing the degree of $g_k^R(x)$ approaching b_k^R , $cc_k^{LR}(x)$ describing the degree of $g_k^L(x)$ approaching b_k^R .

Supposing that $cc_k^{RL}(x)$ monotonously increases from 0 to 1 when boundary $g_k^R(x)$ is approaching b_k^L under the condition that $g_k^R(x) \geq b_k^L - b_k^W$ and there is $cc_k^{RL}(x) \equiv 1$ when $g_k^R(x) \geq b_k^L$, the formula for calculating $cc_k^{RL}(x)$ is derived as (14). It is obvious that there is $cc_k^{RL}(x) \equiv 1$ for all the relative positional relationships between $G_k(x)$ and B_k except the case in Fig. 1(a).

$$cc_k^{RL}(x) = \max \left(0, \frac{g_k^R(x) - (b_k^L - b_k^W)}{b_k^W + |b_k^L - g_k^R(x)|} \right) \quad (14)$$

Supposing that $cc_k^{LL}(x)$ monotonously increases from 0 to 1 when boundary $g_k^L(x)$ is approaching b_k^L under the condition that $g_k^R(x) \geq b_k^L$ and there is $cc_k^{LL}(x) \equiv 1$ when $g_k^L(x) \geq b_k^L$, the formula for calculating $cc_k^{LL}(x)$ can be derived as (15). It is obvious that there is $cc_k^{LL}(x) \equiv 0$ for the relative positional relationship in Fig. 1(a) and $cc_k^{LL}(x) \equiv 1$ for those shown in Figs. 1(c₂), (d), (e).

$$cc_k^{LL}(x) = \max \left(0, \frac{g_k^R(x) - b_k^L}{g_k^R(x) - g_k^L(x) + |b_k^L - g_k^L(x)|} \right) \quad (15)$$

Supposing that $cc_k^{RR}(x)$ monotonously increases from 0 to 1 when boundary $g_k^R(x)$ is approaching b_k^R under the condition that $g_k^R(x) \geq b_k^L$ and there is $cc_k^{RR}(x) \equiv 1$ when $g_k^R(x) \geq b_k^R$, the formula for calculating $cc_k^{RR}(x)$ can be derived as (16). It is obvious that there is $cc_k^{RR}(x) \equiv 0$ for the relative positional relationship in Fig. 1(a) and $cc_k^{RR}(x) \equiv 1$

for those in Figs. 1(c₁), (d), (e).

$$cc_k^{RR}(x) = \max \left(0, \frac{g_k^R(x) - b_k^L}{b_k^R - b_k^L + |b_k^R - g_k^R(x)|} \right) \quad (16)$$

Supposing that $cc_k^{LR}(x)$ monotonously increases from 0 to 1 when boundary $g_k^L(x)$ is approaching b_k^R under the condition that $g_k^R(x) \geq b_k^R$ and there is $cc_k^{LR}(x) \equiv 1$ when $g_k^L(x) \geq b_k^R$, the formula for calculating $cc_k^{LR}(x)$ can be derived as (17). It is obvious that there is $cc_k^{LR}(x) \equiv 0$ for the relative positional relationships in Figs. 1(a), (b), (c₂) and $cc_k^{LR}(x) \equiv 1$ for the case in Fig. 1(e).

$$cc_k^{LR}(x) = \max \left(0, \frac{g_k^R(x) - b_k^R}{g_k^R(x) - g_k^L(x) + |b_k^R - g_k^L(x)|} \right) \quad (17)$$

The variation curves of four closeness coefficients with $g_k^R(x)$ are illustrated in Fig. 2, where Fig. 2(a) corresponds to the case when $g_k^W(x) < b_k^W$ while Fig. 2(b) corresponds to the case when $g_k^W(x) > b_k^W$. It is worth noting that the variation curve of $cc_k^{LL}(x)$ will coincide with that of $cc_k^{RR}(x)$ when $g_k^W(x) = b_k^W$.

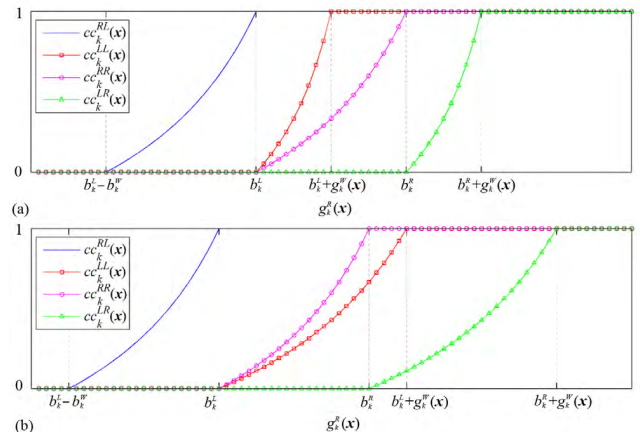


FIGURE 2. Variation curves of four closeness coefficients with $g_k^R(x)$: (a) $g_k^W(x) < b_k^W$; (b) $g_k^W(x) > b_k^W$.

As can be observed from Figs. 1 and 2, the interval constraint $G_k(x) \leq B_k$ will be violated when $g_k^R(x) > b_k^L$, and the larger closeness coefficients $cc_k^{LL}(x)$, $cc_k^{RR}(x)$, $cc_k^{LR}(x)$ indicate the greater violation degree of the interval constraint. Considering that the denominators of the formulae for calculating $cc_k^{LL}(x)$, $cc_k^{RR}(x)$, $cc_k^{LR}(x)$ may be zero when $G_k(x)$ or B_k degenerates into a real number, let $cc_k^{LL}(x) = 0$ when $g_k^L(x) = g_k^R(x) = b_k^L$, $cc_k^{RR}(x) = 0$ when $b_k^L = b_k^R = g_k^R(x)$, and $cc_k^{LR}(x) = 0$ when $g_k^L(x) = g_k^R(x) = b_k^R$. Then the feasibility of interval constraint $G_k(x) \leq B_k$ for design vector x can be assessed by the following tri-dimensional violation vector:

$$v_k(x) = \left(cc_k^{LL}(x), cc_k^{RR}(x), cc_k^{LR}(x) \right),$$

where

$$\begin{aligned}
 & cc_k^{LL}(\mathbf{x}) \\
 &= \begin{cases} 0, & \text{when } \text{sign}(|g_k^L(\mathbf{x}) - g_k^R(\mathbf{x})| + |g_k^L(\mathbf{x}) - b_k^L|) = 0; \\ \max\left(0, \frac{g_k^R(\mathbf{x}) - b_k^L}{g_k^R(\mathbf{x}) - g_k^L(\mathbf{x}) + |b_k^L - g_k^L(\mathbf{x})|}\right), & \text{otherwise.} \end{cases} \\
 & cc_k^{RR}(\mathbf{x}) \\
 &= \begin{cases} 0, & \text{when } \text{sign}(|b_k^L - b_k^R| + |g_k^R(\mathbf{x}) - b_k^R|) = 0; \\ \max\left(0, \frac{g_k^R(\mathbf{x}) - b_k^L}{b_k^R - b_k^L + |b_k^R - g_k^R(\mathbf{x})|}\right), & \text{otherwise.} \end{cases} \\
 & cc_k^{LR}(\mathbf{x}) \\
 &= \begin{cases} 0, & \text{when } \text{sign}(|g_k^L(\mathbf{x}) - g_k^R(\mathbf{x})| + |g_k^L(\mathbf{x}) - b_k^R|) = 0; \\ \max\left(0, \frac{g_k^R(\mathbf{x}) - b_k^L}{g_k^R(\mathbf{x}) - g_k^L(\mathbf{x}) + |b_k^R - g_k^L(\mathbf{x})|}\right), & \text{otherwise.} \end{cases}
 \end{aligned} \tag{18}$$

Therefore, the feasibility of design vector \mathbf{x} for an uncertain mechatronic component can be assessed by the following total tri-dimensional violation vector of all interval constraints in (8):

$$\mathbf{v}_T(\mathbf{x}) = \sum_{k=1}^{ng} \mathbf{v}_k(\mathbf{x}). \tag{19}$$

Design vector \mathbf{x} is feasible if there is $\mathbf{v}_T(\mathbf{x}) = (0, 0, 0)$; otherwise, it is infeasible. Then all the design vectors of an uncertain mechatronic component can be classified into feasible and infeasible ones. A feasible design vector is obviously superior to an infeasible one. The infeasible design vectors can be ranked according to their total tri-dimensional violation vectors calculated by (19). The larger norm of the total tri-dimensional violation vector indicates the worse infeasible design vector.

B. RANKING OF FEASIBLE DESIGN VECTORS CONSIDERING ROBUST EQUILIBRIUM

To achieve the optimal design vector of the heterogeneous-objective robust optimization model in (8), all the feasible design vectors are firstly classified into four groups according to the robust equilibrium among all of their objective and constraint performance indices, then sorted by group according to the preferential relations among different groups, and sorted in each group based on the integral nominal robustness distances of heterogeneous objective performance indices. As a result, the rank orders of all the feasible design vectors can be determined according to their merits of heterogeneous objectives and the robust equilibrium among all structural performance indices.

1) GROUPING AND GROUP RANKING BASED ON ROBUST EQUILIBRIUM STRATEGY

Considering that both the smaller closeness coefficient $cc_k^{RL}(\mathbf{x})$ and the smaller fluctuation of constraint performance index $g_k^W(\mathbf{x})$ will lead to the better robustness of interval constraint $G_k(\mathbf{x}) \leq B_k$, the robust level of constraint performance index $G_k(\mathbf{x})$ can be assessed by the following constraint robustness index:

$$Rg_k(\mathbf{x}) = \max\left\{0, \frac{|g_k^C(\mathbf{x})| - cc_k^{RL}(\mathbf{x}) \times b_k^W}{|g_k^C(\mathbf{x})| + g_k^W(\mathbf{x})}\right\}. \tag{20}$$

It is obvious that constraint robustness index $Rg_k(\mathbf{x})$ takes a value between 0 and 1. The larger constraint robustness index $Rg_k(\mathbf{x})$ indicates the better robustness of constraint performance index $G_k(\mathbf{x})$.

Then the robust equilibrium coefficient for design vector \mathbf{x} corresponding to the k th constraint performance index can be calculated by:

$$Bg_k(\mathbf{x}) = Rg_k(\mathbf{x}) - |b_k^C| / (|b_k^C| + b_k^W), \quad k = 1, 2, \dots, ng. \tag{21}$$

The constraint performance indices are robust equilibrium for design vector \mathbf{x} if there is $\forall Bg_k(\mathbf{x}) \geq 0$; otherwise, they are not. Design vector \mathbf{x}_1 has more robust equilibrium constraint performance indices than design vector \mathbf{x}_2 if there is $\forall Bg_k(\mathbf{x}_1) \geq 0$ but $\exists Bg_k(\mathbf{x}_2) < 0$.

Then all the feasible design vectors can be classified into four groups based on their robust equilibrium coefficients corresponding to all the objective and constraint performance indices calculated by (13) and (21). Specifically, feasible design vector \mathbf{x} belongs to Group A when $\forall Bg_k(\mathbf{x}) \geq 0$ and $\forall Bf_{ji}(\mathbf{x}) \geq 0$; it belongs to Group B when $\forall Bg_k(\mathbf{x}) \geq 0$ but $\exists Bf_{ji}(\mathbf{x}) < 0$; it belongs to Group C when $\forall Bf_{ji}(\mathbf{x}) \geq 0$ but $\exists Bg_k(\mathbf{x}) < 0$; it belongs to Group D when $\exists Bg_k(\mathbf{x}) < 0$ and $\exists Bf_{ji}(\mathbf{x}) < 0$. The preferential relations for the four groups of feasible design vectors are {Group A} > {Group B} > {Group C} > {Group D}.

2) RANKING IN THE SAME GROUP BASED ON ROBUSTNESS DISTANCE

To directly rank the feasible design vectors in the same group, a new concept of robustness distance is proposed. Firstly, a unified formula for calculating the robustness distances of heterogeneous objective performance indices is derived based on the formulae corresponding to the cost, fixation, benefit and deviation ones. Secondly, a dimensionless rank vector is generated for every feasible design vector based on its robustness distances corresponding to heterogeneous objectives. Finally, the integral nominal robustness distances of feasible design vectors are calculated considering the robust equilibrium among all the structural performance indices, based on which the feasible design vectors in the same group can be directly ranked.

For a cost performance index $F_{1i}(\mathbf{x})$, the smaller $f_{1i}^C(\mathbf{x})$ the better, thus its robustness distance can be calculated by:

$$D_{1i}(\mathbf{x}) = [1 - Bf_{1i}(\mathbf{x})] \times f_{1i}^C(\mathbf{x}). \quad (22)$$

For a fixation performance index $F_{2i}(\mathbf{x})$, the smaller $|f_{2i}^C(\mathbf{x}) - b_{2i}^C|$ the better, thus its robustness distance can be calculated by:

$$D_{2i}(\mathbf{x}) = [1 - Bf_{2i}(\mathbf{x})] \times |f_{2i}^C(\mathbf{x}) - b_{2i}^C|. \quad (23)$$

For a benefit performance index $F_{3i}(\mathbf{x})$, the larger $f_{3i}^C(\mathbf{x})$ the better, thus its robustness distance can be calculated by:

$$D_{3i}(\mathbf{x}) = -[1 + Bf_{3i}(\mathbf{x})] \times f_{3i}^C(\mathbf{x}). \quad (24)$$

For a deviation performance index $F_{4i}(\mathbf{x})$, the larger $|f_{4i}^C(\mathbf{x}) - b_{4i}^C|$ the better, thus its robustness distance can be calculated by:

$$D_{4i}(\mathbf{x}) = -[1 + Bf_{4i}(\mathbf{x})] \times |f_{4i}^C(\mathbf{x}) - b_{4i}^C|. \quad (25)$$

Based on (22)-(25), the formula for calculating the robustness distances of heterogeneous objective performance indices can be unified as:

$$D_{ji}(\mathbf{x}) = \text{sign}(2.5 - j) \times [1 - \text{sign}(2.5 - j) \times Bf_{ji}(\mathbf{x})] \times \left(f_{ji}^C(\mathbf{x}) / |f_{ji}^C(\mathbf{x})| \right)^j \times |f_{ji}^C(\mathbf{x}) - b_{ji}^C|. \quad (26)$$

Obviously, the smaller robustness distance $D_{ji}(\mathbf{x})$ indicates the better design vector \mathbf{x} as far as the i th objective performance index of category j is concerned.

Considering that heterogeneous objective performance indices may have different dimensions and different orders of magnitude, the robustness distances calculated by (26) are incommensurable for different objective performance indices. To achieve a dimensionless robustness measure for heterogeneous objectives, all the feasible design vectors in the same group are ranked in parallel according to their corresponding robustness distance $D_{ji}(\mathbf{x})$ to the effect that a smaller robustness distance $D_{ji}(\mathbf{x})$ is assigned a smaller rank number $r_{ji}(\mathbf{x})$ and that feasible design vector \mathbf{x} is assigned a $nf = n1 + n2 + n3 + n4$ dimensional rank vector $\mathbf{r}(\mathbf{x})$ comprising nf number of $r_{ji}(\mathbf{x})$, the norm of which can be calculated by:

$$|\mathbf{r}(\mathbf{x})| = \sqrt{\sum_{i=1}^{n1} r_{1i}(\mathbf{x})^2 + \sum_{i=1}^{n2} r_{2i}(\mathbf{x})^2 + \sum_{i=1}^{n3} r_{3i}(\mathbf{x})^2 + \sum_{i=1}^{n4} r_{4i}(\mathbf{x})^2}. \quad (27)$$

It is obvious that $|\mathbf{r}(\mathbf{x})|$ is a dimensionless quantity reflecting both the merits of heterogeneous objective performance indices and the robust equilibrium among them.

Considering that there is a competition between the constraint and objective performance indices and that the closeness coefficient $cc_k^{RL}(\mathbf{x})$ monotonously increases from 0 to 1 while the constraint robustness index $Rg_k(\mathbf{x})$ monotonously

decreases when $g_k^R(\mathbf{x})$ gradually approaches $b_k^L(\mathbf{x})$, the closeness coefficients $cc_k^{RL}(\mathbf{x})$ is utilized to assess the robust equilibrium between the constraint and objective performance indices. Therefore, the integral nominal robustness distance of design vector \mathbf{x} can be calculated by:

$$D(\mathbf{x}) = \left(2 - \sqrt{\sum_{k=1}^{ng} cc_k^{RL}(\mathbf{x})^2 / \sqrt{ng}} \right) \times |\mathbf{r}(\mathbf{x})|. \quad (28)$$

It is obvious that the smaller integral nominal robustness distance indicates the better and more robust design vector.

V. INTERVAL HETEROGENEOUS-OBJECTIVE ROBUST EQUILIBRIUM OPTIMIZATION ALGORITHM

For the purpose of achieving the globally robust optimal solution to the optimization model in (8), an interval heterogeneous-objective robust equilibrium optimization algorithm is proposed by integrating the Kriging technique for efficiently computing the performance indices of uncertain mechatronic components, the inner GAs for calculating the interval bounds of performance indices, and the outer GA for directly sorting various design vectors based on the preferential guidelines proposed in Section IV. The validity the proposed algorithm is verified by a numerical example.

A. ALGORITHM DESCRIPTION

The flowchart of the interval heterogeneous-objective robust equilibrium optimization algorithm for complex uncertain mechatronic components is illustrated in Fig. 3, the implementation of which includes 6 steps.

Step 1: Construct the interval heterogeneous-objective robust optimization model of the uncertain mechatronic component. Determine the design variables and interval parameters as well as their varying ranges, describe the cost, fixation, benefit and deviation performance indices as heterogeneous objective functions, and describe the requirements on the other performance indices as constraint functions.

Step 2: Construct the Kriging models for efficiently calculating the structural performance indices of the uncertain mechatronic component based on Latin hypercube sampling (LHS) and finite element analysis (FEA).

Step 3: Initialize GA parameters, including the population sizes, maximum iteration numbers, crossover and mutation probabilities of the inner and outer GAs, prescribe the convergent threshold of outer GA. Set the iteration number of outer GA as 1 and generate the first population of outer GA.

Step 4: Calculate the interval bounds of all performance indices in parallel by integrating Kriging models and inner GAs, and calculate the total tri-dimensional violation vectors of all interval constraints for the individuals in the current population of outer GA.

Step 5: Sort the individuals in the current population of outer GA based on the preferential guidelines for design vectors proposed in Section IV, to the effect that the individual corresponding to design vector \mathbf{x} is assigned a rank number $R(\mathbf{x})$. The better and more robust design vector is assigned a

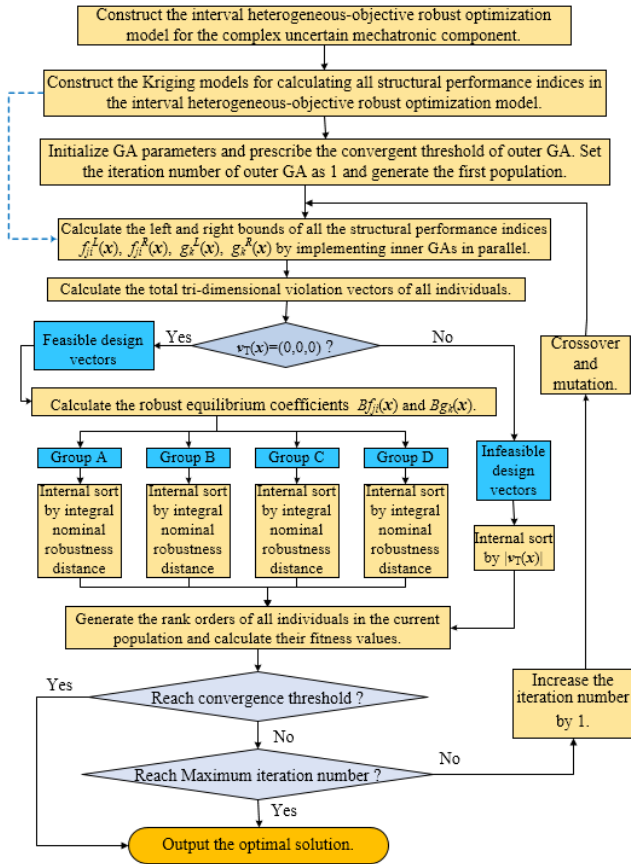


FIGURE 3. Flowchart of the interval heterogeneous-objective robust equilibrium optimization algorithm.

smaller rank number. Then the fitnessvalue of design vector x can be calculated by $Fit(x) = 1/R(x)$.

Step 6: Output the design vector with the largest fitness value as the optimal solution if the outer GA reaches the convergent threshold or maximum iteration number; otherwise, increase the iteration number of outer GA by 1 and generate the next population, return to Step 4.

B. VERIFICATION OF ALGORITHM BY A NUMERICAL EXAMPLE

The numerical example in (29) is utilized to verify the validity of the proposed interval heterogeneous-objective robust equilibrium optimization algorithm. There are the cost, fixation, benefit and deviation objective functions $f_{11}(x, U)$, $f_{21}(x, U)$, $f_{31}(x, U)$ and $f_{41}(x, U)$ in the optimization problem. The interval constant for fixation objective function $f_{21}(x, U)$ to approach is $B_{21} = [4, 8] = \langle 6, 4 \rangle$ while the interval constant for deviation objective function $f_{41}(x, U)$ to deviate from is $B_{41} = [16, 20] = \langle 18, 4 \rangle$. There are two interval constraint functions $g_1(x, U)$ and $g_2(x, U)$ with the same given interval constant of $[0, 0.3]$.

$$\min_x \left\{ \left| \text{sign}(2.5 - j) \times \left(\frac{f_{j1}^C(x)}{f_{j1}^C(x)} \right)^j \times \left| f_{j1}^C(x) - b_{j1}^C \right|, f_{j1}^W(x) \right| \right\}$$

where

$$\begin{aligned} f_{j1}^C(x) &= (f_{j1}^L(x) + f_{j1}^R(x))/2, \quad f_{j1}^W(x) = f_{j1}^R(x) - f_{j1}^L(x); \\ f_{j1}^L(x) &= \min_U f_{j1}(x, U), \\ f_{j1}^R(x) &= \max_U f_{j1}(x, U), \quad (j = 1, 2, 3, 4) \\ \langle b_{11}^C, b_{11}^W \rangle &= \langle b_{31}^C, b_{31}^W \rangle = \langle 0, 0 \rangle, \quad \langle b_{21}^C, b_{21}^W \rangle = \langle 6, 4 \rangle, \\ \langle b_{41}^C, b_{41}^W \rangle &= \langle 18, 4 \rangle; \\ f_{11}(x, U) &= U_1^2(x_1 - 1)^2/4 - U_2^2(x_2 - 4)^2/2; \\ f_{21}(x, U) &= U_1^2(x_1^2 + x_1x_2 + 1) + U_2(x_1x_2 - x_1^2 - 2); \\ f_{31}(x, U) &= U_1^3(x_1 + x_2^2) - U_2(x_2 + 2)^2; \\ f_{41}(x, U) &= U_1(x_1 + x_2 - 7.5)^2 + U_2^2(x_2 - x_1 + 3)^2; \\ \text{s.t. } g_1(x, U) &= U_1^2(x_1 - 2)^3/2 + U_2x_2 - 2.5 \leq [0, 0.3]; \\ g_2(x, U) &= U_1^3x_2 + U_2^2x_1 - 3.85 \\ &\quad - 8U_2^2(x_2 - x_1 + 0.65)^2 \leq [0, 0.3]. \\ x_1 &\in [0, 5], x_2 \in [0, 3]; \\ U_1 &= [0.9, 1.1], \quad U_2 = [0.9, 1.1]. \end{aligned} \tag{29}$$

There is no need to construct Kriging models here since all the objective and constraint functions in (29) are analytical. The maximum iteration number, population size, crossover and mutation probabilities are 150, 100, 0.99 and 0.05 respectively for both the inner and outer GAs for solving the numerical example. Besides the maximum iteration number given as the stop criterion, the outer GA iteration is terminated when the absolute differences of $f_{j1}^C(x)$ between the optimal solution and the average of the current population are less than 10^{-2} . The outer GA reaches the convergent threshold after 68 iterations and achieves the optimal solution $x^0 = (1.20, 2.26)$. The convergent curves of the heterogeneous objectives and constraints obtained by the proposed algorithm are illustrated in Fig. 4 and Fig. 5 respectively.

To solve the numerical example in (29) by conventional optimization algorithm [49], it should be transformed into a single objective unconstrained deterministic model at first based on the weighting and penalty function methods. The weighting factors of $f_{j1}^C(x)$, $f_{j1}^W(x)$ ($j = 1, 2, 3, 4$) are settled as 1/8 with the same normalization factor of 1 while the penalty factors and satisfactory degrees for both constraints are prescribed as 1000 and 1 respectively. Then the model after transformation is solved by the nested GA with the same GA parameters and convergent threshold as those utilized in the proposed method. The outer GA converges at the 36th generation, with the optimal solution located as $x^* = (3.61, 0.00)$. Table 1 lists the statistics of the heterogeneous objectives and constraints in (29) at the optimal solutions obtained by the proposed and indirect algorithms. As can be seen from Table 1, both constraints $g_1(x^0, U)$ and $g_2(x^0, U)$ are fully satisfied at x^0 obtained by the proposed algorithm but constraint $g_1(x^*, U)$ will be violated at x^* obtained by the indirect algorithm, which leads to the small robustness index

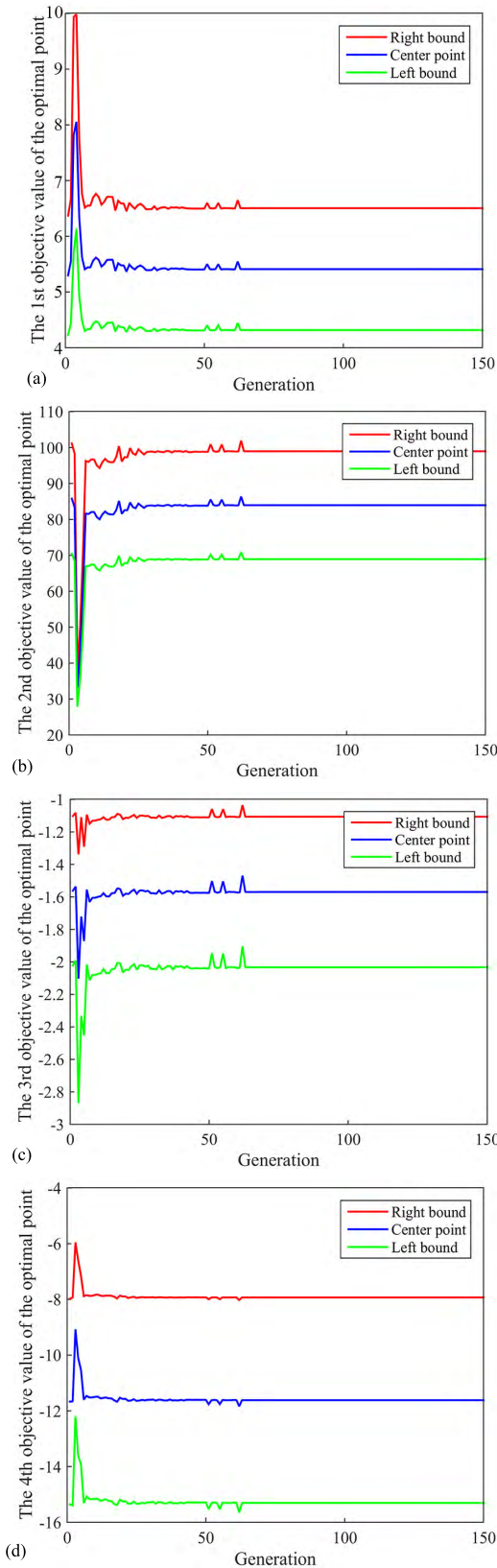


FIGURE 4. Convergent curves of the objective values: (a) The 1st objective value of the optimal point; (b) The 2nd objective value of the optimal point; (c) The 3rd objective value of the optimal point; (d) The 4th objective value of the optimal point.

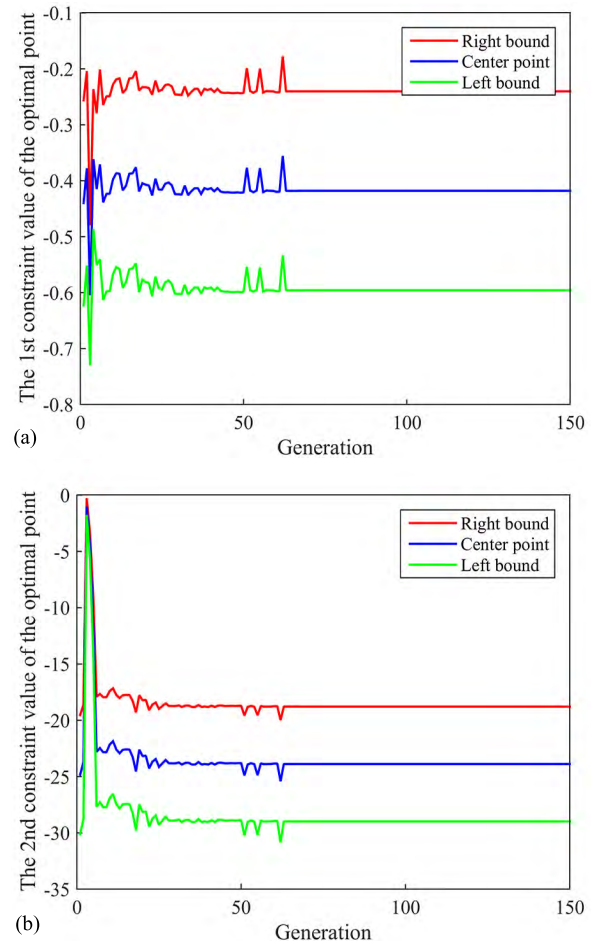


FIGURE 5. Convergent curves of constraint values: (a) The 1st constraint value of the optimal point; (b) The 2nd constraint value of the optimal point.

of 0.33. Meanwhile, the interval of the fixation objective function $f_{21}(\mathbf{x}^0, \mathbf{U})$ ($[4.37, 6.57]$) at \mathbf{x}^0 is fully enclosed by its corresponding interval constant $[4, 8]$ while that of $f_{21}(\mathbf{x}^*, \mathbf{U})$ ($[-5.17, 3.45]$) is not, which also leads to the small robustness index of 0.40 for the fixation objective function at \mathbf{x}^* . To sum up, the robustness indices of all the objective and constraint functions range from 0.53 to 0.77 at the optimal solution \mathbf{x}^0 obtained by the proposed algorithm while those at the optimal solution \mathbf{x}^* obtained by the indirect algorithm range from 0.08 to 0.78, demonstrating that the proposed algorithm can achieve the optimal solution with much more robust equilibrium objective and constraint values to the heterogeneous-objective robust optimization problem in (29) than the indirect one. Additionally, the experience-depended model transformation process in the indirect algorithm has also been avoided.

VI. CASE STUDY

A. PROBLEM DESCRIPTION

The high-speed stamping press illustrated in Fig. 6 (a) is a kind of complex mechatronic equipment capable of continuously stamping various motor cores, such as those

TABLE 1. Heterogeneous-objective robust optimization results of the numerical example in (29).

| Method | Statistics | Heterogeneous objective functions | | | | Constraint functions | |
|----------|---------------------------|-----------------------------------|----------------|-----------------|----------------|----------------------|------------------|
| | | $f_{11}(x, U)$ | $f_{21}(x, U)$ | $f_{31}(x, U)$ | $f_{41}(x, U)$ | $g_1(x, U)$ | $g_2(x, U)$ |
| Proposed | [Left bound, Right bound] | [-2.01, -1.09] | [4.37, 6.57] | [-15.37, -7.94] | [68.96, 99.02] | [-0.57, -0.22] | [-29.10, -18.85] |
| | <Center, Width> | <-1.55, 0.92> | <5.47, 2.20> | <-11.65, 7.43> | <83.99, 30.06> | <-0.40, 0.35> | <-23.98, 10.25> |
| | Robustness index | 0.62 | 0.77 | 0.61 | 0.72 | 0.53 | 0.70 |
| Indirect | [Left bound, Right bound] | [-9.27, -3.77] | [-5.17, 3.45] | [-1.77, 1.20] | [13.36, 16.48] | [-1.07, 0.02] | [-84.20, -57.64] |
| | <Center, Width> | <-6.52, 5.50> | <-0.86, 8.61> | <-0.28, 2.97> | <14.92, 3.12> | <-0.52, 1.08> | <-70.92, 26.56> |
| | Robustness index | 0.54 | 0.40 | 0.08 | 0.78 | 0.33 | 0.73 |

utilized in new energy vehicles, air-conditioning compressors, and so on. The high-speed actuating mechanism in Fig. 6 (b) is the most important component of a stamping press, the structural performance indices of which greatly influence the stamping precision of press and the service life of molds. According to the research results of previous work [47], [48], the frictional heat generated at the ten bearings for connecting the crankshaft with linkages or upper beam will lead to the significant temperature rise and thermal deformation of the actuating mechanism in the stamping process. Therefore, the frictional heat as well as its influence on structural performance indices should be considered in the robust optimization of the high-speed actuating

mechanism. Considering that the larger rotary speed of crankshaft will lead to the larger frictional heat at the bearings, both the geometrical parameters b_1, b_2, b_3, h in Fig. 6(c) and the rotary speed of crankshaft n are chosen as design variables. The density ρ and Poisson ratio ν of slider are described as interval numbers considering their uncertainties. The varying ranges of five design variables and two interval parameters are listed in Table 2. There are $b_1 = 85\text{mm}$, $b_2 = 30\text{mm}$, $b_3 = 30\text{mm}$, $h = 980\text{mm}$, $n = 400\text{rpm}$ for the initial design of the high-speed actuating mechanism.

Considering that the thermal stiffness of slider is the most important performance index for the high-speed actuating mechanism, the maximum thermal deformation of slider indicating thermal stiffness is described as the objective performance index, which is a cost objective function of interval parameters ρ and ν . The stamping frequency of press is also chosen as the objective function considering its influence on the production efficiency and the temperature rise in the actuating mechanism, which is a benefit one independent of uncertain parameters. To avoid ponderous and risky design, the upper limits for the weight and maximum thermal equivalent stress of the slider are prescribed as [1400, 1500] kg and [200, 210] MPa respectively, which are described as constraint functions. The weight of slider is independent of Poisson ratio ν and thus it is only influenced by interval density ρ . The maximum thermal equivalent stress of the slider is the function of both interval Poisson ratio ν and interval density ρ . Consequently, the interval heterogeneous-objective robust optimization model for the high-speed actuating mechanism can be constructed as

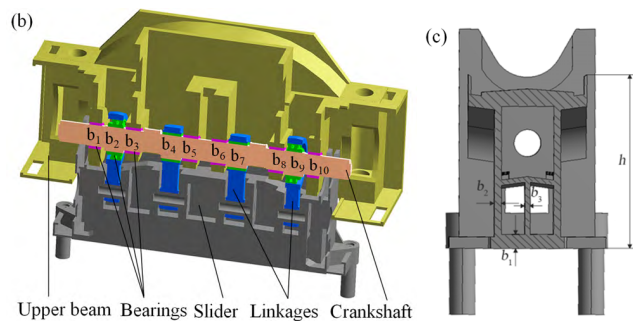
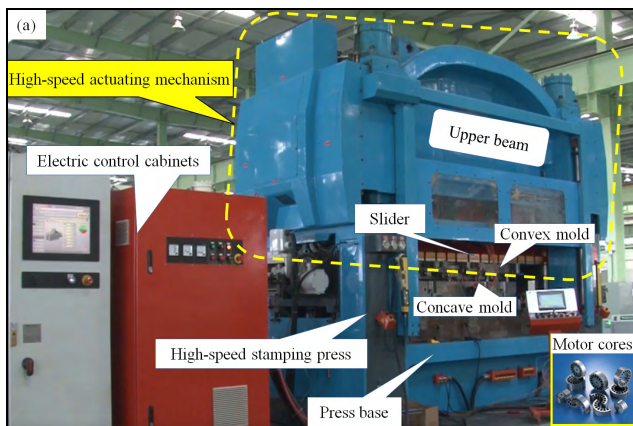


FIGURE 6. The high-speed stamping press: (a) photo of a workplace; (b) 1/2 solid model of the high-speed actuating mechanism; (c) cross section of slider.

$$\min_x \{d(x, U), -f_s(n)\}$$

where

$$d(x, U) = [d^L(x), d^R(x)] = \langle d^C(x), d^W(x) \rangle;$$

$$d^L(x) = \min_U d(x, U), \quad d^R(x) = \max_U d(x, U);$$

$$d^C(x) = (d^L(x) + d^R(x))/2,$$

$$d^W(x) = d^R(x) - d^L(x).$$

$$\text{s.t. } w(x, U_1) = [w^L(x), w^R(x)] \leq [1400, 1500]\text{kg};$$

TABLE 2. Varying ranges of design variables and uncertain parameters.

| | b_1 (mm) | b_2 (mm) | b_3 (mm) | h (mm) | n (rpm) | ρ (kg/mm ³) | ν |
|---------|------------|------------|------------|----------|-----------|------------------------------|-------|
| Minimum | 50 | 20 | 15 | 880 | 250 | 7200 | 0.27 |
| Maximum | 120 | 40 | 50 | 1120 | 450 | 7400 | 0.33 |

$$\delta(\mathbf{x}, \mathbf{U}) = [\delta^L(\mathbf{x}), \delta^R(\mathbf{x})] \leq [200, 210]\text{MPa};$$

$$w^L(\mathbf{x}) = \min_{U_1} w(\mathbf{x}, U_1), w^R(\mathbf{x}) = \max_{U_1} w(\mathbf{x}, U_1);$$

$$\delta^L(\mathbf{x}) = \min_U \delta(\mathbf{x}, \mathbf{U}), \delta^R(\mathbf{x}) = \max_U \delta(\mathbf{x}, \mathbf{U}). \quad (30)$$

where $\mathbf{x} = (b_1, b_2, b_3, h, n)$ is the design vector, $\mathbf{U} = (U_1, U_2) = (\rho, \nu)$ is the interval parameter vector; $d(\mathbf{x}, \mathbf{U})$ is the maximum thermal deformation of slider while $d^L(\mathbf{x}), d^R(\mathbf{x}), d^C(\mathbf{x})$ and $d^W(\mathbf{x})$ are its left bound, right bound, center and width; $f_s(n)$ is the stamping frequency of the press and there is $f_s(n) = n$ for the investigated high-speed press; $w(\mathbf{x}, U_1)$ and $\delta(\mathbf{x}, \mathbf{U})$ are the weight and maximum thermal equivalent stress of slider while $w^L(\mathbf{x}), w^R(\mathbf{x}), \delta^L(\mathbf{x}), \delta^R(\mathbf{x})$ are their left and right bounds respectively.

B. CONSTRUCTION OF KRIGING MODELS

It is cumbersome and computationally expensive to calculate the high-speed actuating mechanism’s structural performance indices considering the influence of frictional heat since the thermal loads and boundary conditions need to be calculated for design vectors with different rotary speed of the crankshaft. Therefore, three Kriging models need to be constructed for calculating the maximum thermal deformation $d(\mathbf{x}, \mathbf{U})$, weight $w(\mathbf{x}, U_1)$ and maximum thermal equivalent stress $\delta(\mathbf{x}, \mathbf{U})$ of the slider in order to solve the robust optimization model in (30). The sample points for constructing Kriging models are generated by LHS in the space determined by the design variables and interval parameters, with the structural performance indices of which obtained by FEA. The force loads and constraints of the finite element model are illustrated in Fig. 7. The thermal loads and boundary conditions of the initial design $\mathbf{x}^1 = (85, 30, 30, 980, 400)$ are illustrated in Fig. 8 while the thermal deformation and thermal equivalent stress of the initial design when $\mathbf{U} = (7300, 0.3)$ are illustrated in Fig. 9.

The construction of Kriging models is an iterative process [14]. Specifically, the initial Kriging models for calculating the maximum thermal deformation $d(\mathbf{x}, \mathbf{U})$, weight $w(\mathbf{x}, U_1)$ and maximum thermal equivalent stress $\delta(\mathbf{x}, \mathbf{U})$ of the slider are constructed by 164 sample points generated by LHS. Then 10 test points generated by LHS are utilized to verify the prediction precision of the current Kriging models based on the calculation of multiple correlation coefficient (MCC) and relative maximum absolute error (RMAE). The test points as well as 3 resampled points arranged around every current sample point of the largest RMAE are added to the sample point set to construct the next Kriging models when there exists $MCC < 0.95$ or

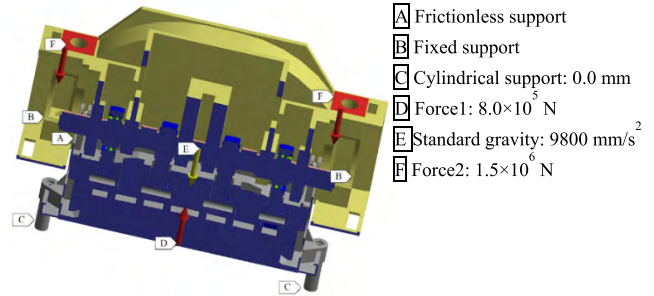


FIGURE 7. Force loads and constraints of the 1/2 finite element model.

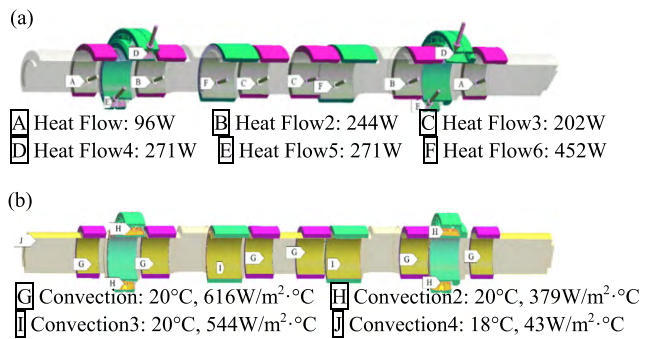
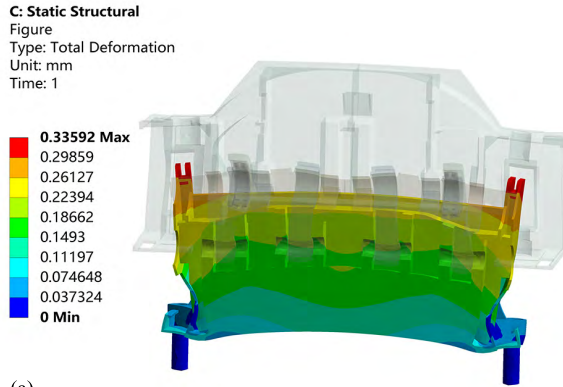


FIGURE 8. Finite element model of the initial design: (a) thermal loads; (b) boundary conditions.

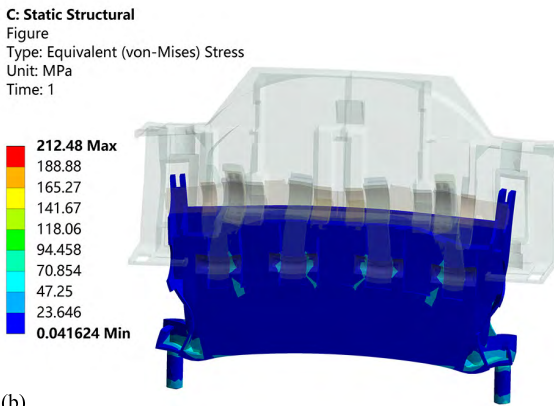
RMAE>0.05. The statistics of the Kriging models in the iteration process are listed in Table 3. The statistical data in the last line of Table 3 demonstrate that all of the three Kriging models generated by 252 sample points can satisfy the requirement of prediction precision and thus can be utilized to calculate the structural performance indices of the slider in the heterogeneous-objective robust optimization process.

C. OPTIMIZATION RESULTS AND DISCUSSIONS

The interval heterogeneous-objective robust optimization model in (30) is solved by the proposed algorithm integrating Kriging models with nested GA, the parameters of which are listed in Table 4. The outer GA evolution is terminated when the absolute differences of $d^C(\mathbf{x}), f_s(n)$ between the optimal solution and the average of the current population are less than 10^{-4} mm and 1rpm respectively. As can be seen from the convergent curves of the structural performance indices in Fig. 10, the outer GA reaches the convergent threshold after 70 iterations and the optimal design vector is obtained as $\mathbf{x}^0 = (116.8, 29.2, 18.9, 1015.6, 259.0)$.



(a)

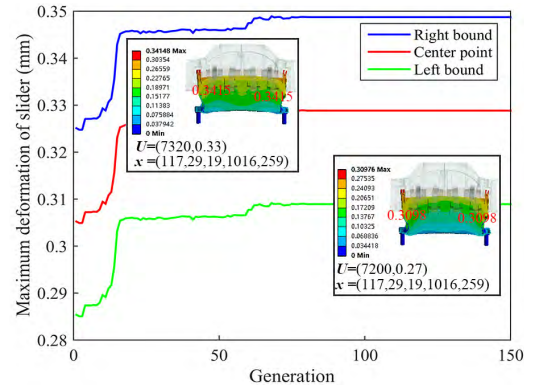


(b)

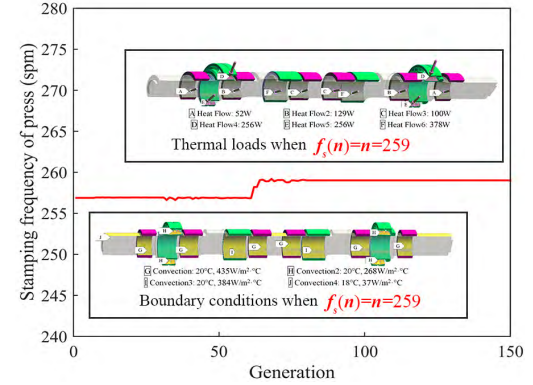
FIGURE 9. Structural performance indices of the initial design when $U=(7300, 0.3)$: (a) thermal deformation; (b) thermal equivalent stress.

To solve the optimization model in (30) by conventional indirect algorithm [49], it is transformed into a single objective unconstrained deterministic model at first based on the weighting and penalty function methods. The weighting factors of $d^C(x)$, $d^W(x)$, $f_s(n)$ are settled as 1/3 while their normalization factors are settled as 0.001, 0.00008 and 1 respectively. The penalty factors and satisfactory degrees for both constraints are prescribed as 1000 and 1 respectively. Then the model after transformation is solved by the nested GA with the same GA parameters and convergent threshold as those utilized in the proposed method. The outer GA converges at the 16th generation, with the optimal solution located as $x^*=(110.5, 40.0, 42.2, 1053.6, 254.5)$.

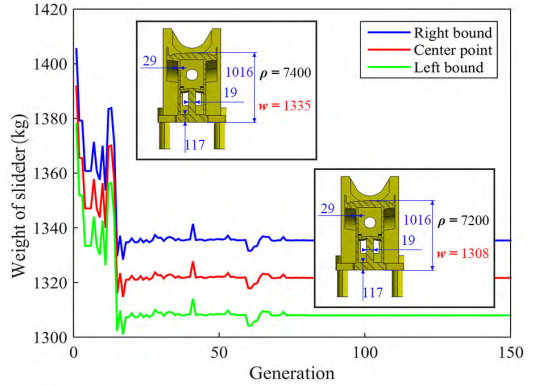
Table 5 provides a comparison of the structural performance indices of the optimal design obtained by the proposed and indirect algorithms. As can be seen from Table 5, the width of the maximum thermal deformation at the optimal solution x^0 obtained by the proposed algorithm is smaller than that at x^* obtained by the indirect one although the center of the maximum thermal deformation at x^0 is slightly larger than that at x^* , leading to the improvement of objective robustness index of maximum thermal deformation. At the same time,



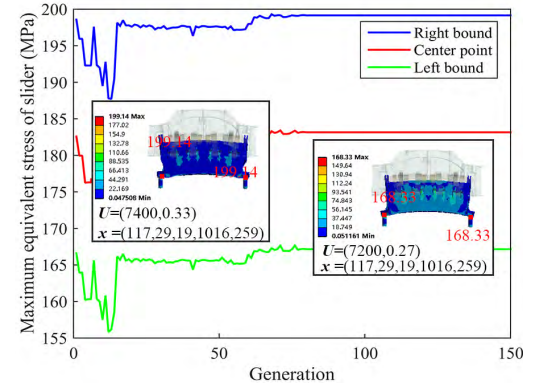
(a)



(b)



(c)



(d)

FIGURE 10. Convergent curves of structural performance indices: (a) maximum deformation of slider; (b) stamping frequency of press; (c) weight of slider; (d) maximum equivalent stress of slider.

TABLE 3. Statistics of the Kriging models for computing the structural performance indices of the slider.

| Iterations | Number of sample points | $d(x, U)$ | | $w(x, U_i)$ | | $\delta(x, U)$ | |
|------------|-------------------------|-----------|--------|-------------|--------|----------------|--------|
| | | R^2 | RMAE | R^2 | RMAE | R^2 | RMAE |
| 0 | 164 | 0.6245 | 0.4436 | 0.6079 | 0.4672 | 0.8719 | 0.3060 |
| 1 | 189 | 0.6848 | 0.4418 | 0.8056 | 0.3457 | 0.9015 | 0.1231 |
| 2 | 211 | 0.8654 | 0.2629 | 0.8846 | 0.1977 | 0.9821 | 0.0818 |
| 3 | 230 | 0.9864 | 0.0690 | 0.9746 | 0.0949 | 0.9965 | 0.0445 |
| 4 | 252 | 0.9976 | 0.0265 | 0.9979 | 0.0231 | 0.9967 | 0.0372 |

TABLE 4. GA parameters for solving the interval heterogeneous-objective robust optimization model in (30).

| GA | Maximum iteration number | Population size | Crossover probability | Mutation probability |
|----------|--------------------------|-----------------|-----------------------|----------------------|
| Inner GA | 100 | 150 | 0.99 | 0.05 |
| Outer GA | 150 | 150 | 0.99 | 0.05 |

TABLE 5. Comparison of the structural performance indices of the actuating mechanism obtained by different methods.

| Method | Statistics | Objective performance indices | | Constraint performance indices | |
|----------|---------------------------|-------------------------------|--------------|--------------------------------|--------------------|
| | | $d(x, U)$ mm | $f_s(n)$ spm | $w(x, U_i)$ kg | $\delta(x, U)$ MPa |
| Proposed | [Left bound, Right bound] | [0.3089, 0.3487] | 259 | [1308.0, 1335.4] | [167.2, 199.1] |
| | <Center, Width> | <0.3288, 0.0399> | <259, 0> | <1321.7, 27.4> | <183.2, 31.9> |
| | Robustness index | 0.8918 | 1 | 0.9638 | 0.8129 |
| Indirect | [Left bound, Right bound] | [0.2848, 0.3248] | 255 | [1328.8, 1356.2] | [165.1, 209.1] |
| | <Center, Width> | <0.3053, 0.0410> | <255, 0> | <1342.5, 27.4> | <187.1, 44> |
| | Robustness index | 0.8816 | 1 | 0.9515 | 0.7663 |

the benefit performance index of stamping frequency at x^0 obtained by the proposed algorithm is higher than that at x^* obtained by the indirect one with the same robustness index of 1. Both constraints of weight and maximum thermal equivalent stress are fully satisfied at the optimal solution x^0 obtained by the proposed algorithm while the constraint on maximum equivalent stress may be violated at the optimal solution x^* obtained by the indirect one. Thus, the proposed algorithm can achieve the optimal solution with more robust constraints than the indirect one, which can also be observed from the larger robustness indices of the weight and maximum equivalent stress corresponding to x^0 in comparison with those corresponding to x^* . To sum up, the proposed algorithm can achieve the optimal solution with the more robust equilibrium structural performance indices than the indirect one since the maximum difference among the robustness indices of all structural performance indices corresponding to x^0 (0.1871) is smaller than that corresponding to x^* (0.2337).

Although the indirect approach might also achieve a solution with both constraints satisfied by adjusting the penalty factors of constraints in the model transformation process, it is dependent on the rich experience of engineering designers. Similarly, different normalization factors for the heterogeneous objectives in Eq. (30) will also produce different optimization results, the determination of their appropriate values is also dependent on the experience of engineering designers. Whereas the proposed approach can directly locate the optimal solution to the interval heterogeneous objective robust optimization model based on the direct ranking of design vectors according to the robust equilibrium strategy among the heterogeneous objectives and constraints

so that the high-challenging model transformation process can be avoided. Therefore, the effectiveness and advantage of the proposed heterogeneous-objective robust optimization approach in the design optimization of complex mechatronic components with interval uncertainties are demonstrated.

VII. CONCLUSION

This paper proposed the new research topic of the robust parameter optimization of complex mechatronic components involving heterogeneous competing objectives for the first time. A unified interval heterogeneous-objective robust optimization model was constructed for complex uncertain mechatronic components considering the probable coexistence of the cost, fixation, benefit and deviation performance indices. The unified formulae for assessing the robustness of heterogeneous objective performance indices and the robust equilibrium among them were proposed. The preferential guidelines for ranking various design vectors were put forward based on grouping and group ranking considering the robust equilibrium among all of the structural performance indices. Subsequently, an integrated interval robust equilibrium optimization algorithm was proposed to achieve the optimal solution to the heterogeneous-objective robust optimization model of uncertain mechatronic components, which efficiently computed the structural performance indices by Kriging models, calculated in parallel the interval bounds of structural performance indices by a series of inner GAs, and directly sorted alternative design vectors in the outer GA according to the preferential guidelines considering the robust equilibrium among all structural performance indices. The validity of the proposed optimization algorithm as well

as its advantage over previous indirect one was verified by a numerical example with the cost, fixation, benefit and deviation objectives. Finally, a case study on the high-speed actuating mechanism in a stamping press is conducted. The aim is to minimize the thermal deformation and maximize the stamping frequency under the restrictions on the weight and maximum equivalent stress. The optimization results demonstrated that the proposed approach could not only ensure the fully satisfaction of both constraints on the weight and maximum equivalent stress but also achieve the more robust structural performance indices than the indirect approach. The proposed approach also demonstrated its obvious advantage of convenient implementation by avoiding the high-challenging model transformation process.

In this paper, the interval robust equilibrium optimization algorithm is developed to locate a single optimal solution for the interval heterogeneous-objective robust optimization problem and avoid the challenging decision making process of choosing the final design after optimization. Future research may focus on the development of multi-objective optimization algorithm for solving the interval heterogeneous-objective robust optimization problems so as to provide a group of trade off solutions for the conflicting cost, fixation, benefit and deviation objectives.

REFERENCES

- [1] L. Wang, W. Sun, Y. Long, and X. Yang, "Reliability-based performance optimization of tunnel boring machine considering geological uncertainties," *IEEE Access*, vol. 6, pp. 19086–19098, 2018.
- [2] J. Feng, D. Wu, W. Gao, and G. Li, "Hybrid uncertain natural frequency analysis for structures with random and interval fields," *Comput. Methods Appl. Mech. Eng.*, vol. 328, pp. 365–389, Jan. 2018.
- [3] L. Wang, W. Sun, Y. Long, and X. Yang, "Reliability-based performance optimization of tunnel boring machine considering geological uncertainties," *IEEE Access*, vol. 9, pp. 19086–19098, 2018.
- [4] M. G. Villarreal-Cervantes, A. Rodríguez-Molina, C. García-Mendoza, O. Peñaloza-Mejía, and G. Sepúlveda-Cervantes, "Multi-objective on-line optimization approach for the DC motor controller tuning using differential evolution," *IEEE Access*, vol. 5, pp. 20393–20407, 2017.
- [5] V. Gabrel, C. Murat, and A. Thiele, "Recent advances in robust optimization: An overview," *Eur. J. Oper. Res.*, vol. 235, no. 3, pp. 471–483, Jun. 2014.
- [6] J. C. Yu, and S. Suprayitno, "Evolutionary reliable regional Kriging surrogate and soft outer array for robust engineering optimization," *IEEE Access*, vol. 5, pp. 16520–16531, 2017.
- [7] N. Yorino, M. Abdillahi, Y. Sasaki, and Y. Zoka, "Robust power system security assessment under uncertainties using Bi-level optimization," *IEEE T. Power Syst.*, vol. 33, no. 1, pp. 352–362, Jan. 2018.
- [8] M. Jansen, G. Lombaert, and M. Schevenels, "Robust topology optimization of structures with imperfect geometry based on geometric nonlinear analysis," *Comput. Methods Appl. Mech. Eng.*, vol. 285, pp. 452–467, Mar. 2015.
- [9] X. Peng, J. Li, S. Jiang, and Z. Liu, "Robust topology optimization of continuum structures with loading uncertainty using a perturbation method," *Eng. Optim.*, vol. 50, no. 4, pp. 584–598, 2018.
- [10] D. Wu, W. Gao, K. Gao, and F. Tin-Loi, "Robust safety assessment of functionally graded structures with interval uncertainties," *Compos. Struct.*, vol. 180, pp. 664–685, Nov. 2017.
- [11] X. Y. Long, C. Jiang, X. Han, W. Gao, X. G. Wang, and M. Z. Hou, "Probabilistic crack trajectory analysis by a dimension reduction method," *Fatigue Fract. Eng. Mater. Struct.*, vol. 40, no. 1, pp. 12–26, 2017.
- [12] J. C. Medina and A. Taflanidis, "Probabilistic measures for assessing appropriateness of robust design optimization solutions," *Struct. Multidisciplinary Optim.*, vol. 51, no. 4, pp. 813–834, 2015.
- [13] J. N. Richardson, R. F. Coelho, and S. Adriaenssens, "Robust topology optimization of truss structures with random loading and material properties: A multiobjective perspective," *Comput. Struct.*, vol. 154, pp. 41–47, Jul. 2015.
- [14] J. Cheng, Z. Liu, Z. Wu, X. Li, and J. Tan, "Robust optimization of structural dynamic characteristics based on adaptive Kriging model and CNSGA," *Struct. Multidisciplinary Optim.*, vol. 51, no. 2, pp. 423–437, 2015.
- [15] J. Martínez-Frutos, D. Herrero-Pérez, M. Kessler, and F. Periago, "Robust shape optimization of continuous structures via the level set method," *Comput. Methods Appl. Mech. Eng.*, vol. 305, pp. 271–291, Jun. 2016.
- [16] W. Zhang and Z. Kang, "Robust shape and topology optimization considering geometric uncertainties with stochastic level set perturbation," *Int. J. Numer. Methods Eng.*, vol. 110, no. 1, pp. 31–56, 2017.
- [17] C. Jiang, B. Y. Ni, X. Han, and Y. R. Tao, "Non-probabilistic convex model process: A new method of time-variant uncertainty analysis and its application to structural dynamic reliability problems," *Comput. Methods Appl. Mech. Eng.*, vol. 268, pp. 656–676, Jan. 2014.
- [18] J. L. Wu, Z. Luo, N. Zhang, and Y. Q. Zhang, "A new interval uncertain optimization method for structures using Chebyshev surrogate models," *Comput. Struct.*, vol. 146, pp. 185–196, Jun. 2015.
- [19] C. Yang, Z. Lu, and Z. Yang, "Robust optimal sensor placement for uncertain structures with interval parameters," *IEEE Sensors J.*, vol. 18, no. 5, pp. 2031–2041, Mar. 2018.
- [20] D. Wu and W. Gao, "Uncertain static plane stress analysis with interval fields," *Int. J. Numer. Meth. Engng.*, vol. 110, pp. 1272–1300, 2017.
- [21] T. Kernicky, M. Whelan, U. Rauf, and E. Al-Shaer, "Structural identification using a nonlinear constraint satisfaction processor with interval arithmetic and contractor programming," *Comput. Struct.*, vol. 188, pp. 1–16, 2017.
- [22] M. Faes, J. Cerneels, D. Vandepitte, and D. Moens, "Identification and quantification of multivariate interval uncertainty in finite element models," *Comput. Methods Appl. Mech. Eng.*, vol. 110, pp. 1272–1300, Jun. 2017.
- [23] B. Y. Ni, C. Jiang, and Z. L. Huang, "Discussions on non-probabilistic convex modelling for uncertain problems," *Appl. Math. Model.*, vol. 59, pp. 54–85, Jul. 2018.
- [24] L. Xie, J. Liu, G. Huang, W. Zhu, and B. Xia, "A polynomial-based method for topology optimization of phononic crystals with unknown-but-bounded parameters," *Int. J. Numer. Methods Eng.*, vol. 144, no. 7, pp. 777–800, 2018.
- [25] C. M. Fu, L. X. Cao, J. C. Tang, and X. Y. Long, "A subinterval decomposition analysis method for uncertain structures with large uncertainty parameters," *Comput. Struct.*, vol. 197, pp. 58–69, Feb. 2018.
- [26] J. Cheng, Z. Y. Liu, J. R. Tan, Y. Y. Zhang, M. Y. Tang, and G. F. Duan, "Optimization of uncertain structures with interval parameters considering objective and feasibility robustness," *Chin. J. Mech. Eng.*, vol. 31, no. 38, pp. 1–13, 2018.
- [27] Y. Han, D. Gong, Y. Jin, and Q. K. Pan, "Evolutionary multi-objective blocking lot-streaming flow shop scheduling with interval processing time," *Appl. Soft Comput.*, vol. 42, pp. 229–245, May 2016.
- [28] D. Gong, J. Sun, and Z. Miao, "A set-based genetic algorithm for interval many-objective optimization problems," *IEEE Trans. Evol. Comput.*, vol. 22, no. 1, pp. 47–60, Feb. 2018.
- [29] J. Sun, D. Gong, X. Zeng, and N. Geng, "An ensemble framework for assessing solutions of interval programming problems," *Inf. Sci.*, vols. 436–437, pp. 146–161, Apr. 2018.
- [30] J. Zhou, S. Cheng, and M. Li, "Sequential quadratic programming for robust optimization with interval uncertainty," *J. Mech. Des.*, vol. 134, no. 10, pp. 1–13, 2012.
- [31] A. Mortazavi, S. Azarm, and S. A. Gabriel, "Adaptive gradient-assisted robust design optimization under interval uncertainty," *Eng. Optim.*, vol. 45, no. 11, pp. 1287–1307, 2013.
- [32] S. Cheng, J. Zhou, and M. Li, "A new hybrid algorithm for multi-objective robust optimization with interval uncertainty," *J. Mech. Des.*, vol. 137, no. 2, p. 021401, 2015.
- [33] J. Wu, J. Gao, Z. Luo, and T. Brown, "Robust topology optimization for structures under interval uncertainty," *Adv. Eng. Softw.*, vol. 99, pp. 36–48, Sep. 2016.
- [34] X. Chen, J. Fan, and X. Bian, "Structural robust optimization design based on convex model," *Results Phys.*, vol. 7, pp. 3068–3077, 2017.
- [35] A. Hot, T. Weisser, and S. Cogan, "An info-gap application to robust design of a prestressed space structure under epistemic uncertainties," *Mech. Syst. Signal Process.*, vol. 91, pp. 1–9, Jul. 2017.

- [36] R. W. Hanks, J. D. Weir, and B. J. Lunday, "Robust goal programming using different robustness echelons via norm-based and ellipsoidal uncertainty sets," *Eur. J. Oper. Res.*, vol. 262, pp. 636–646, Oct. 2017.
- [37] J. Cheng, Z. Liu, M. Tang, and J. Tan, "Robust optimization of uncertain structures based on normalized violation degree of interval constraint," *Comput. Struct.*, vol. 182, pp. 41–54, Apr. 2017.
- [38] N. Hu, B. Duan, H. Cao, and Y. Zong, "Robust optimization with convex model considering bounded constraints on performance variation," *Struct. Multidisciplinary Optim.*, vol. 56, no. 1, pp. 59–69, 2017.
- [39] J. Liu and H. C. Gea, "Robust topology optimization under multiple independent unknown-but-bounded loads," *Comput. Methods Appl. Mech. Eng.*, vol. 329, pp. 464–479, Feb. 2018.
- [40] Q. Zhou, P. Jiang, X. Y. Shao, H. Zhou, and J. X. Hu, "An on-line Kriging metamodel assisted robust optimization approach under interval uncertainty," *Eng. Comput.*, vol. 34, no. 2, pp. 420–446, 2017.
- [41] Q. Zhou et al., "A multi-objective robust optimization approach for engineering design under interval uncertainty," *Eng. Comput.*, vol. 35, no. 2, pp. 580–603, 2018.
- [42] Q. Zhou, P. Jiang, X. Huang, F. Zhang, and T. Zhou, "A multi-objective robust optimization approach based on Gaussian process model," *Struct. Multidisciplinary Optim.*, vol. 57, no. 1, pp. 213–233, 2018.
- [43] D. Gong and J. Yuan, "Large population size IGA with individuals' fitness not assigned by user," *Appl. Soft Comput.*, vol. 11, pp. 936–945, Jan. 2011.
- [44] D. Gong, G. Guo, L. Lu, and H. Ma, "Adaptive interactive genetic algorithms with individual interval fitness," *Prog. Natural Sci.*, vol. 18, no. 3, pp. 359–365, 2008.
- [45] J. Cheng, Y. Feng, Z. Lin, Z. Liu, and J. Tan, "Anti-vibration optimization of the key components in a turbo-generator based on heterogeneous axiomatic design," *J. Cleaner Prod.*, vol. 141, pp. 1467–1477, Jan. 2017.
- [46] J. Cheng, Y. Zhang, Y. Feng, Z. Liu, and J. Tan, "Structural optimization of a high-speed Press considering multi-source uncertainties based on a new heterogeneous TOPSIS," *Appl. Sci.*, vol. 8, no. 1, p. 126, 2018.
- [47] J. Cheng, Z. Zhou, Z. Liu, Y. Zhang, and J. Tan, "Thermo-mechanical coupling analysis of a high-speed actuating mechanism based on a new thermal contact resistance model," *Appl. Therm. Eng.*, vol. 140, pp. 487–497, Jul. 2018.
- [48] J. Cheng, Z. Zhou, Y. Feng, Z. Liu, and Y. Zhang, "Thermo-mechanical coupling analysis of the actuating mechanism in a high speed Press," *Int. J. Precis. Eng. Manuf.*, vol. 19, no. 5, pp. 643–653, 2018.
- [49] C. Jiang, X. Han, and G. R. Liu, "Optimization of structures with uncertain constraints based on convex model and satisfaction degree of interval," *Comput. Methods Appl. Mech. Eng.*, vol. 196, pp. 4791–4800, Nov. 2007.



YANGMING QIAN received the B.Eng. degree in mechanical engineering from Southeast University, Nanjing, China, in 2017. He is currently pursuing the M.S. degree with the School of Mechanical Engineering, Zhejiang University, China. His current research interests include the uncertainty modeling of engineering problems and the robust optimization of complex structures.



ZHENYU LIU received the Ph.D. degree in mechanical engineering from Zhejiang University, Hangzhou, China, in 2002, where he is currently a Professor with the State Key Laboratory of CAD&CG. His research interests include CAD, virtual prototyping, virtual-reality-based simulation, and robotics.



YIXIONG FENG (M'17) received the B.S. and M.S. degrees in mechanical engineering from Yanshan University, Qinhuangdao, China, in 1997 and 2000, respectively, and the Ph.D. degree in mechanical engineering from Zhejiang University, Hangzhou, China, in 2004, where he is currently a Professor with the Department of Mechanical Engineering and also a member of the fluid power and mechatronic systems. His research focuses on mechanical product design theory, intelligent automation, and advance manufacture technology.



ZHENDONG ZHOU received the B.Eng. degree in mechanical engineering from the Hefei University of Technology, Hefei, China, in 2015, and the M.S. degree in mechanical engineering from Zhejiang University, Hangzhou, China, in 2018. His research interests include the uncertainty modeling of engineering problems and the robust optimization of complex structures.



JIANRONG TAN received the M.S. degree in engineering and the Ph.D. degree in science from Zhejiang University, Hangzhou, China, where he is currently a Professor with the State Key Laboratory of Fluid Power and Mechatronic Systems. He is also an Academician of the Chinese Academy of Engineering. His research interests include CAD&CG, mechanical design and theory, and digital design and manufacture.



JIN CHENG received the Ph.D. degree in mechanical engineering from Zhejiang University, China, in 2005, where she is currently an Associate Professor with the Department of Mechanical Engineering and also a member of the State Key Laboratory of Fluid Power and Mechatronic Systems. Her research interests include the uncertainty modeling of engineering problems, the uncertainty optimization of complex structures, and the intelligent design of complex equipment.

...